MODELING OF ENERGY DISSIPATION SUBSIDIARY PIERS FOR A LONG SPAN CABLE-STAYED BRIDGE

Limin Sun*† and Jun Wei

State Key Laboratory of Disaster Reduction in Civil Engineering, Tongji University, China

ABSTRACT

China has been planning several sea-crossing projects consisting of long span cable-stayed bridges. Because of long natural periods, the bridges locating at seismic areas may respond to large displacement, and suffer from severe damage on structural components or even collapse under strong earthquake. Because the seismic performance of long cable-stayed bridges is mainly dependent on structural system, it is significant to investigate the damage mechanisms and its control of long cable-stayed bridges with different systems subjected to strong ground motion.

Based on the elastic-plastic analyses results of the entire model of a trial designed cable-stayed bridge with a main span of 1400 m and two towers of 365 m high, new structural systems considering damage control strategies of sacrificing subsidiary piers have been proposed by the authors. According to the seismic demands of the subsidiary piers redesigned following the strategies proposed, three types of 1/10 scaled RC subsidiary piers models have been design and tested under a cyclical reversed horizontal load. All models tested are rectangular hollow reinforced concrete columns. One is a single column, the others are twin-columns linked by energy dissipation members which are shear links (SLs) or buckling restrained braces (BRBs).

In this paper, based on the experimental results, constitutive models for the energy dissipation members were developed. By using the models developed, elasto-plastic analyses for energy dissipation piers were conducted, and the simulations can estimate well the elastic stiffness, the yielding strength as well as the hysteresis of the subsidiary piers. The same modelling was employed for the entire cable-stayed bridge structure, the FEM simulation results showed that the subsidiary piers with energy dissipation members can improve the seismic capacity of the bridge significantly.

Keywords: Long cable-stayed bridge, energy dissipation subsidiary piers, modeling, elasto-plastic analyses, shear links, buckling restrained braces.

---

*Corresponding author: Email: lmsun@tongji.edu.cn

†Presenter: Email:lmsun@tongji.edu.cn

1. INTRODUCTION

Strong earthquakes can cause significant damage to long span cable-stayed bridges. It is a key for structural safety to provide reliable energy dissipation mechanisms for bridges under strong earthquakes. Inelastic deformation can limit the forces in structural members for rational design, as well as to provide hysteretic energy dissipation for structural systems. The concept of designing sacrificial members to dissipate the seismic energy, while preserving the integrity of other main components, is well known as the structural damage control concept (Connor et al 1997). Sacrificial members should be easily replaceable secondary members. The previous research work on the structural damage control concept focused on implementation in buildings; recently the same concept is applied in bridge engineering. The quasi-static loading tests were conducted on two prototype steel shear links for the main tower of the new San Francisco-Oakland Bay self-anchored suspension bridge to evaluate the link force and deformation capacities (Mcdaniel et al. 2003). El-Bahey and Bruneau (2011) proposed a design procedure using BRBs as structural fuses for the retrofit of RC bridge bents, which was found to be sufficiently reliable to design structural fuses system with satisfactory seismic performance.

With respect to seismic damage control for long span cable-stayed bridge, a new structural system with a damage control strategy, that the energy dissipation subsidiary piers have been designed to dissipate seismic energy and the tower remained elastic or subjected to minor damage, has been proposed by the authors (Limin Sun and Wen Xie 2010). Based the experimental investigation of the energy dissipation subsidiary pier, this paper will present the analytical model and compare the numerical results with the experimental data. At last the contribution of energy dissipation members to RC columns will be evaluated.

2. EXPERIMENTS

The tested models were three types of 1/10-scaled RC columns with rectangular hollow sections. The height and wall thickness of the hollow column was 6 m and 150 mm, respectively. The first model was a single RC (SRC) column pier (labeled as Model SRC), the cross section of which was 850 mm×1050 mm. The other models were twin-column piers with the cross section of 850 mm× 520 mm. SLs were installed between the two RC columns (TRC) to serve as a series of energy dissipation members on the second model (labeled as Model TRC-SL), while the third model used BRBs as a series of energy dissipation members between the two columns (labeled as Model TRC-BRB). A more detailed description of models can be referenced in the literature (Limin Sun et al. 2012).

The strength degrade of supplied commercial concrete was C30, The measured concrete strength and the elastic modulus values, as shown in Table 1, were obtained using 150 mm×150 mm×150 mm cubes at the test age, which was about 28 days after casting. The material properties of the reinforcing rebar and Q235 steel plate are shown in Table 2.

Table 1: Material properties of concrete

models	Cube compressive strength (MPa)	Elastic modulus ($\times10^4$MPa)
SRC	32.4	3.06
TRC-SL	35.4	3.14
TRC-BRB	33.0	3.08

Table 2: Material properties of reinforcing rebar and Q235 steel plate

Steel grades	Diameter or thickness（mm）	Yielding strength (MPa)	Ultimate strength (MPa)	Elongation (%)
HPB300	10	338	462	30
HRB335	12	364	538	31
Q235	5	275	386	-
Q235	6	304	420	-
Q235	10	285	444	-

3. FINIT ELEMENT MODELING

Finite element models replicating the behaviors of energy dissipation subsidiary piers were developed with the same geometrical and loading characteristics previously presented using the software OpenSees (Mazzoni S et al. 2007). The 6 m high column was modeled by nine elasto-plastic fiber beam-column elements. The length of four bottom elements is 0.25 m, while the length of other five elements is 1 m. Five integration sections per beam-column element were used. The embedded parts and connection regions were modeled by rigid arm elements. The SL was modeled by shear link element consisting of an elastic beam element and two zero length elements at both ends, and the BRB was modeled by truss element. The finite element models of three subsidiary piers are shown in Figure 1.

3.1. Element models

The fiber beam-column element is illustrated in Figure 2in the local coordinate system x, y and z. The cross section is divided into a discrete number of elements. These sections are located at the control points of the numerical integration. Each section is subdivided into longitudinal fibers. The geometric characteristics of the fiber are its location of local y and z reference system and the fiber area. The constitutive relationship of the section is derived by integration of the response of the fibers, which follow the uniaxial stress - strain relationship of the particular material.

The SL is modeled by a simple and effective link element model (Ramandan and Ghobarah 1995). As shown in Figure 3, four nodes represent the complete element i, i', j, j'. A typical elastic beam element connects the two slaved nodes i' and j'. The length of this element is taken equal to the link length e. The two primary nodes i and j have the same coordinates as the two slaved nodes i' and j'. The distance between each primary and slaved node is equal to zero. The moment hinges occurring at the link ends and the shear hinge occurring along its web are assumed to occur at the primary and slaved nodes. The deformation of the spring element is defined as the relative rotation or translation between the primary nodes and slaved nodes.

The BRB is modeled by a truss element, which only resists the axial force (compression or tension). Furthermore, the cross section of the truss element is divided into longitudinal fibers. The connection region between the energy dissipation member and the RC column is modeled by the rigid arm element.

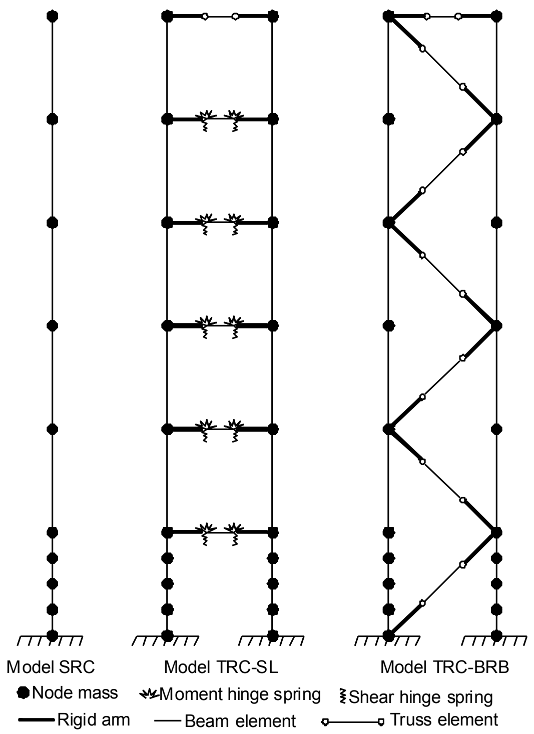

Figure 1: Finite element models

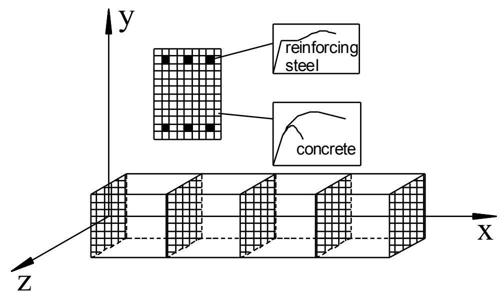

Figure 2: Fiber beam-column element

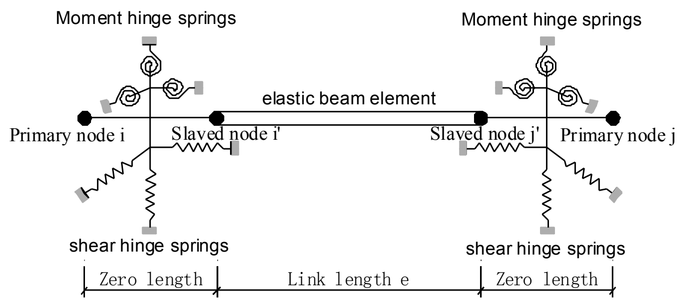

Figure 3: Shear link (SL) element

3.2. Material constitutive model

In what concerns the material constitutive relationship, for the concrete in compression the well known model of Mander (Mander et al. 1988) was adopted, which was a confined concrete model applicable to both circle and rectangular shaped transverse reinforcement. The behavior of concrete in tension was not considered. In order to account for the confinement of the transverse reinforcement, the compression strength and the corresponding strain were modified through the following confinement factor k_c.

$$f_{cc} = k_c f_{c0} \tag{1}$$

$$\varepsilon_{cc} = \varepsilon_{c0}\left[1+5\left(k_c-1\right)\right] \tag{2}$$

The unconfined concrete strain ε_{c0} corresponding the maximum compression strength was taken as

0.02, while the value for the confinement factor was 1.3 for the confined concrete and 1.0 for the cover concrete.

The model of Giuffré, Menegotto and Pinto (1973) was applied for the longitudinal reinforcement steel. The steel modulus of elasticity was taken equal to 200 GPa, while the hardening and cyclic behavior parameters were calibrated in order to better replicate the experimental results: b=0.015, R=12. The model is computationally efficient and agrees well with the experimental results from cyclic tests on reinforcing rebar.

The bilinear model can be used to describe the constitutive relationship of the energy dissipation members. The shear force-deformation relationship is adopted to model the shear hinge spring, while the moment-curvature relationship is adopted to model the moment hinge spring. The yield shear force and moment are 165 kN and 88 kN.mm for the SL respectively, which were computed by equation (3) and (4).

$$V_P = \frac{\sigma_{yw}}{\sqrt{3}} t_w \left(d - 2t_f\right) \tag{3}$$

$$M_P = \sigma_{yf} t_f b \left(d - t_f\right) + \sigma_{yw} t_w \left(\frac{d - 2t_f}{2}\right)^2 \tag{4}$$

Where V_p is the yield shear force for the end section of the SL, M_p is the corresponding yield moment in the presence of shear force for the same section, σ_{yw} is the yield stress of the web plate, σ_{yf} is the yield stress of the flange plate, t_w is the web thickness, d is the section depth, t_f is the flange thickness, and b is the section width.

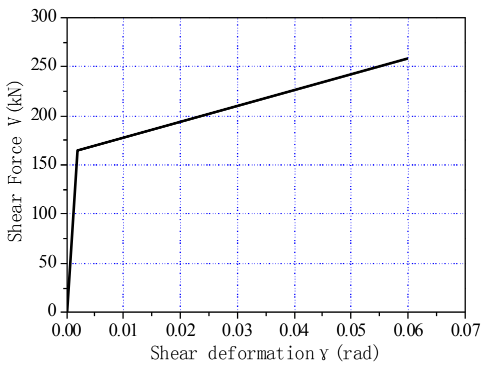

Figure 4: Shear force-deformation relationship of SL

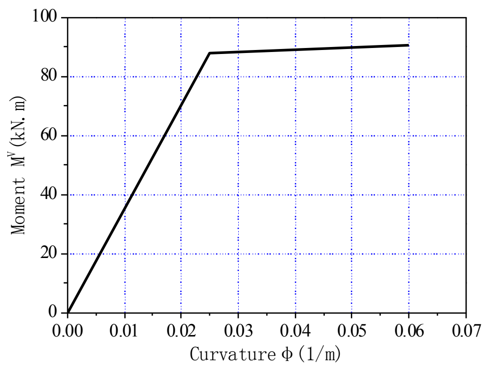

Figure 5: Moment-curvature relationship of SL

The yield shear angle can be calculated by the equation of $\gamma_y = k\frac{V_p}{GA}$. Where k is the section shape factor which results from uneven shear stress distribution on the cross section, for the I-shaped cross section, $k = A / A_w$, A_w is the web cross section area, G is the shear modulus, and A is the cross section area.

The yield curvature can be calculated by the equation of $\phi_y = \frac{M_p}{EI}$. Where E is the elastic modulus; and I is the inertia moment of SL.

Figure 4 and Figure 5 show the shear force - deformation relationship and the moment - curvature relationship of the SL, respectively. The post - yield shear stiffness and flexural stiffness are assumed as0.002 times elastic shear stiffness and flexural stiffness, respectively.

The stress - strain relationship of the low yielding point steel is taken as the constitutive relationship of the fiber of the BRB cross section. The strength measurements are applied in the material constitutive model.

4. COMPARISON BETWEEN EXPERIMENTS AND NUMERICAL MODELS

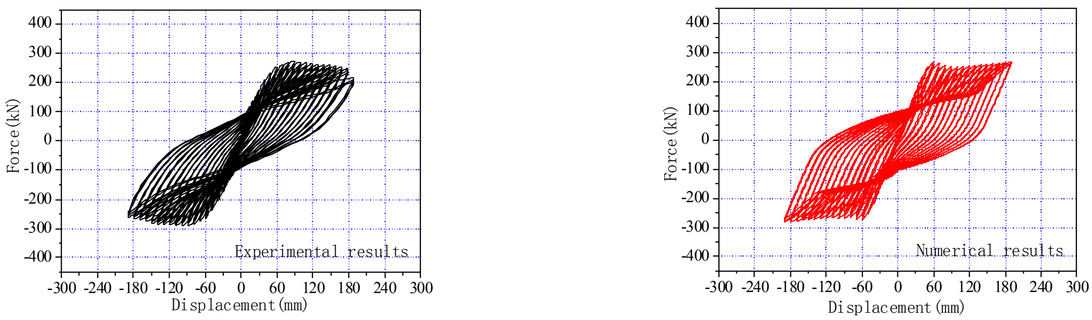

(a) Model SRC

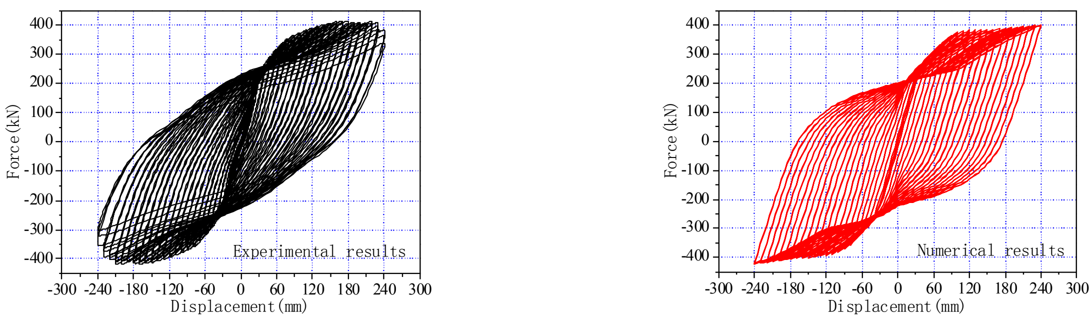

(b) Model TRC-SL

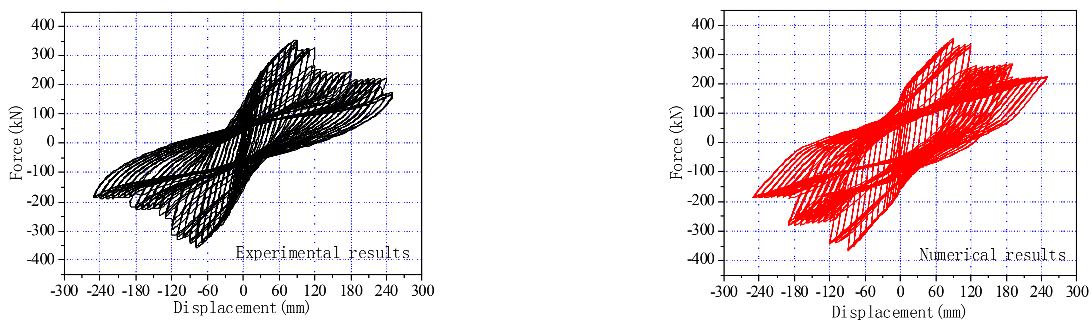

(c) Model TRC-BRB

Figure 6: Comparison of experimental results with numerical models

Figure 6 shows the comparisons of experimental results with numerical analyses for all tested models. It can be seen from the hysteresis loops of top displacement and force of the tested models that the experimental results and numerical analyses match well for all models except the discrepancies of the strength after the columns yielded. The degradation of the strength is not well predicted in the plastic stage of the models.

5. CONTRIBUTION OF ENERGY DISSIPATION MEMBERS TO SEISMIC CAPACITY OF RC COLUMNS

The bare twin-column pier with the energy dissipation members removed from Model TRC-SL and Model TRC-BRB is labeled as Model TRC. The cyclic loading analysis for Model TRC was conducted, and the hysteretic curves of Model TRC are shown in Figure 7. It can be seen that the shape of the hysteretic curves of Model TRC is not as full as the model with the energy dissipation members, and the area surrounded by the hysteretic curves is very small.

The total energy dissipated by the models is equal to the sum of the area surrounded by all hysteretic curves. The pushover analyses for the bare twin-column pier and the twin-column pier with energy dissipation members were performed respectively. The pushover curves of the three models are shown in Figure 8. It can be seen that the contribution of energy dissipation members to the stiffness and strength of the twin-column piers is quite notable. Especially the elastic stiffness and post-yield strength of Model TRC-SL increases by 300 % and 130 % because of the SL added, respectively.

Table 3 shows the contribution of energy dissipation members to energy dissipation capacity of the models. The dissipated energy for Model TRC-SL because of the energy dissipation members (SLs) increases by 520 %, compared with Model TRC. So the contribution of the SL to energy dissipation capacity of the subsidiary pier is very significant. However, the dissipated energy for Model TRC-BRB only increases by 190 % owe to the unexpected failure of the BRBs.

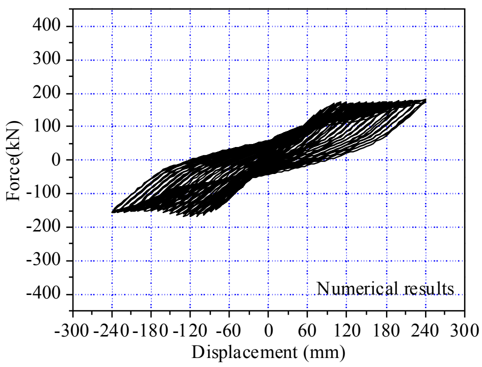

Figure 7: Hysteretic curves of Model TRC

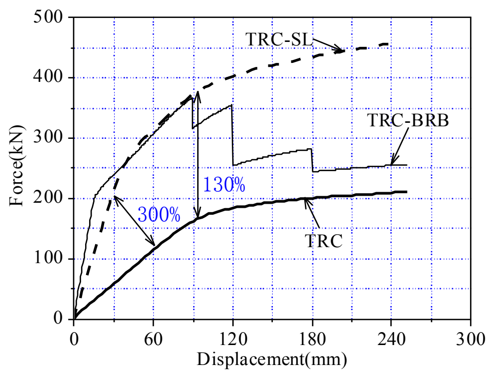

Figure 8: Pushover analysis results

The pushover analyses for the bare twin-column pier and the twin-column pier with energy dissipation members were performed respectively. The pushover curves of the three models are shown in Figure 8. It can be seen that the contribution of energy dissipation members to the stiffness and strength of the twin-column piers is quite notable. Especially the elastic stiffness and post-yield strength of Model TRC-SL increases by 300 % and 130 % because of the SL added, respectively.

Table 3: Contribution of energy dissipation members to energy dissipation capacity of models

Models	Dissipated energy （MN·m）	Dissipated energy increment compared with the bare RC columns （%）
TRC	0.8	-
TRC-SL	4.98	520
TRC-BRB	2.33	190

6. CONCLUSIONS

The modeling of the energy dissipation subsidiary piers for long span cable-stayed bridges was investigated to replicate the full range of results obtained from the experiments and to highlight the difference in behavior between the bare twin-column pier and the twin-column pier with energy dissipation members. Some conclusions can be drawn as follows.

(1) The results of numerical model match well with the experimental results for all tested models except the discrepancies of the strength after the columns yielded. However, the degradation of the strength is not well predicted in the plastic stage of the models.

(2) The numerical simulations show that the contribution of the SL to energy dissipation capacity of the subsidiary pier is very significant. However, the dissipated energy increment for Model TRC-BRB is not large owe to the unexpected failure of the BRBs.

7. ACKNOWLEDGMENTS

The authors wish to thank the financial support provided by National Natural Science Foundation of China (Grant No. 90915011).

REFERENCES

Connor JJ, Wada A, and Iwata M, et al (1997). Damage-controlled structures. I: Preliminary design methodology for seismically active regions. Journal of Structural Engineering - ASCE. 123(4): pp.423-431.

El-Bahey S and Bruneau M (2011). Buckling restrained braces as structural fuses for the seismic retrofit of reinforced concrete bridge bents. Engineering Structures.33(3): pp. 1052-1061.

Limin Sun and Wen Xie (2010). Damage Mechanism and Damage Control of Long Span Cable-stayed Bridges Under Strong Earthquake. Fifth World Conference on Structural Conrol and Monitoring.Tokyo,Japan.

Limin Sun, Jun Wei and Wen Xie (2012). Vulnerability and Damage Control of Long Span Cable-stayed Bridge. First International Conference on Performance-based and Life-cycle Structural Engineering. Hong Kong, China.

Mander JB, Priestley MJN, and Park R (1988). Theoretical stress-strain model for confined concrete. Journal of Structural Engineering-ASCE. 114(8): pp. 1804-1826.

Mazzoni S, McKenna F, Fenves G L (2007). OpenSees Command Language Manual [Z]. Berkeley: PEER, University of California.

Mcdaniel CC, Uang C, andSeible F (2003). Cyclic Testing of Built-Up Steel Shear Links for the New Bay Bridge.Journal of Structural Engineering. 129(6): pp. 801-809.

Menegotto M and Pinto P (1973). Method of analysis for cyclically loaded RC plane frames including changes in geometry and non-elastic behavior of elements under combined normal force and bending. Lisbon.

Ramadan T and Ghobarah A (1995). Analytical Model for Shear-Link Behavior.Journal of Structural Engineering. 121(11): pp. 1574-1580.